

INCIDENCE RATE OF GRB-HOST DLAs AT HIGH REDSHIFT

KENTARO NAGAMINE,^{1,2} BING ZHANG,¹ AND LARS HERNQUIST³

Received 2008 June 17; accepted 2008 September 8; published 2008 September 22

ABSTRACT

We study the incidence rate of damped Ly α systems associated with the host galaxies of gamma-ray bursts (GRB-host DLAs) as functions of neutral hydrogen column density ($N_{\text{H I}}$) and projected star formation rate (SFR) using cosmological SPH simulations. Assuming that the occurrence of GRBs is correlated with the local SFR, we find that the median $N_{\text{H I}}$ of GRB-host DLAs progressively shifts to lower $N_{\text{H I}}$ values with increasing redshift, and the incidence rate of GRB-host DLAs with $\log N_{\text{H I}} > 21.0$ decreases rapidly at $z \geq 6$. Our results suggest that the likelihood of observing the signature of IGM attenuation in GRB afterglows increases toward higher redshift, because it will not be blocked by the red damping wing of DLAs in the GRB host galaxies. This enhances the prospects of using high-redshift GRBs to probe the reionization history of the universe. The overall incidence rate of GRB-host DLAs decreases monotonically with increasing redshift, whereas that of QSO DLAs increases up to $z = 6$. A measurement of the difference between the two incidence rates would enable an estimation of the value of η_{GRB} , which is the mass fraction of stars that become GRBs for a given amount of star formation. Our predictions can be tested by upcoming high- z GRB missions, including *JANUS* (*Joint Astrophysics Nascent Universe Scout*) and *SVOM* (*Space multiband Variable Object Monitor*).

Subject headings: cosmology: theory — galaxies: evolution — galaxies: formation — methods: numerical — stars: formation

Online material: color figures

1. INTRODUCTION

A number of authors have proposed using GRBs to probe the history of cosmic star formation and the reionization of the universe (e.g., Totani 1997; Miralda-Escudé 1998; Lamb & Reichart 2000; Barkana & Loeb 2004), neither of which is well understood (see, e.g., Holder et al. 2003; Nagamine et al. 2006). To date, observations of high-redshift (hereafter high- z) quasars and galaxies have been able to constrain reionization only up to $z \sim 7$ (Fan et al. 2006). However, if GRBs are associated with the deaths of massive stars (e.g., Woosley 1993; Paczyński 1998), then theoretical studies imply that GRBs may be detectable out to $z \approx 10$ – 20 through their prompt γ -ray emission and afterglows (Lamb & Reichart 2000; Ciardi & Loeb 2000; Gou et al. 2004; Inoue et al. 2007). This raises the possibility of using GRBs to investigate the reionization history of the universe, and the *Swift* satellite has indeed detected high- z GRBs with bright afterglows (Cusumano et al. 2006; Haislip et al. 2006; Kawai et al. 2006).

However, GRB lines of sight (LOSs) tend to probe more the inner parts of galaxies than the random QSO LOSs do, and are therefore often associated with neutral hydrogen (H I) absorption (Prochaska et al. 2007). Indeed, analyses of the afterglow spectra reveal the presence of DLAs in the red damping wing (Vreeswijk et al. 2004; Berger et al. 2006; Watson et al. 2006; Ruiz-Velasco et al. 2007), and the DLAs may hide the absorption signatures of the neutral IGM (Totani et al. 2006). If such cases dominate the high- z GRB afterglow spectra, then it may be difficult to use GRBs to probe the detailed reionization history of the universe (McQuinn et al. 2008). Thus, it is important to understand the redshift evolution of the incidence rate of GRB-host DLAs at $z \geq 6$ as a function of $N_{\text{H I}}$.

In this Letter, we use cosmological SPH simulations based on the concordance Λ cold dark matter (CDM) model to study the $N_{\text{H I}}$ distribution and the incidence rate of GRB-host DLAs as a function of redshift between $z = 1$ and 10. The DLAs associated with quasar LOSs are often referred to as QSO DLAs. Since quasars serve as randomly distributed background beacons in the universe, QSO DLAs can be more broadly interpreted as all the H I gas clouds that satisfy the DLA criterion ($N_{\text{H I}} > 2 \times 10^{20} \text{ cm}^{-2}$), regardless of whether or not they have been intersected by quasar LOSs. We adopt the latter broad interpretation of QSO DLAs in this Letter, and by this definition GRB-host DLAs are a subset of QSO DLAs.

2. SIMULATIONS

Our simulations were performed with the smoothed particle hydrodynamics (SPH) code GADGET-2 (Springel 2005), which includes radiative cooling by hydrogen and helium, heating by a uniform UV background (Katz et al. 1996; Davé et al. 1999), star formation and supernova feedback based on a subparticle multiphase ISM model, and a phenomenological description of galactic winds (Springel & Hernquist 2003a, 2003b).

Here, we use the Q5 and G5 runs from Springel & Hernquist (2003b) which have box sizes of 10 and 100 h^{-1} Mpc, respectively. The total particle number is $N_p = 2 \times 324^3$ for gas and dark matter in each run. The initial gas particle mass is $m_{\text{gas}} = 3.3 \times 10^5$ (3.3×10^8) $h^{-1} M_{\odot}$, and the dark matter particle mass is $m_{\text{dm}} = 2.1 \times 10^6$ (2.1×10^9) $h^{-1} M_{\odot}$. The comoving gravitational softening length, a measure of the spatial resolution of the simulation, is 1.2 (8.0) h^{-1} kpc for the Q5 (G5) run. We use the Q5 run for $z > 3$ (for higher resolution), and the G5 run for $z < 3$ (for better sampling of more massive halos and longer wavelength perturbations).

Previously, we have used these simulations to study the properties of DLAs (Nagamine et al. 2004a, 2004b, 2007), Lyman break galaxies at $z = 3$ – 6 (Nagamine et al. 2004c; Night et

¹ University of Nevada, Department of Physics and Astronomy, 4505 Maryland Parkway, Box 454002, Las Vegas, NV 89154-4002; kn@physics.unlv.edu.

² Visiting Researcher, Institute for the Physics and Mathematics of the universe, 5-1-5 Kashiwanoha Kashiwa-shi, Chiba 277-8582, Japan.

³ Harvard University, 60 Garden Street, Cambridge, MA 02138.

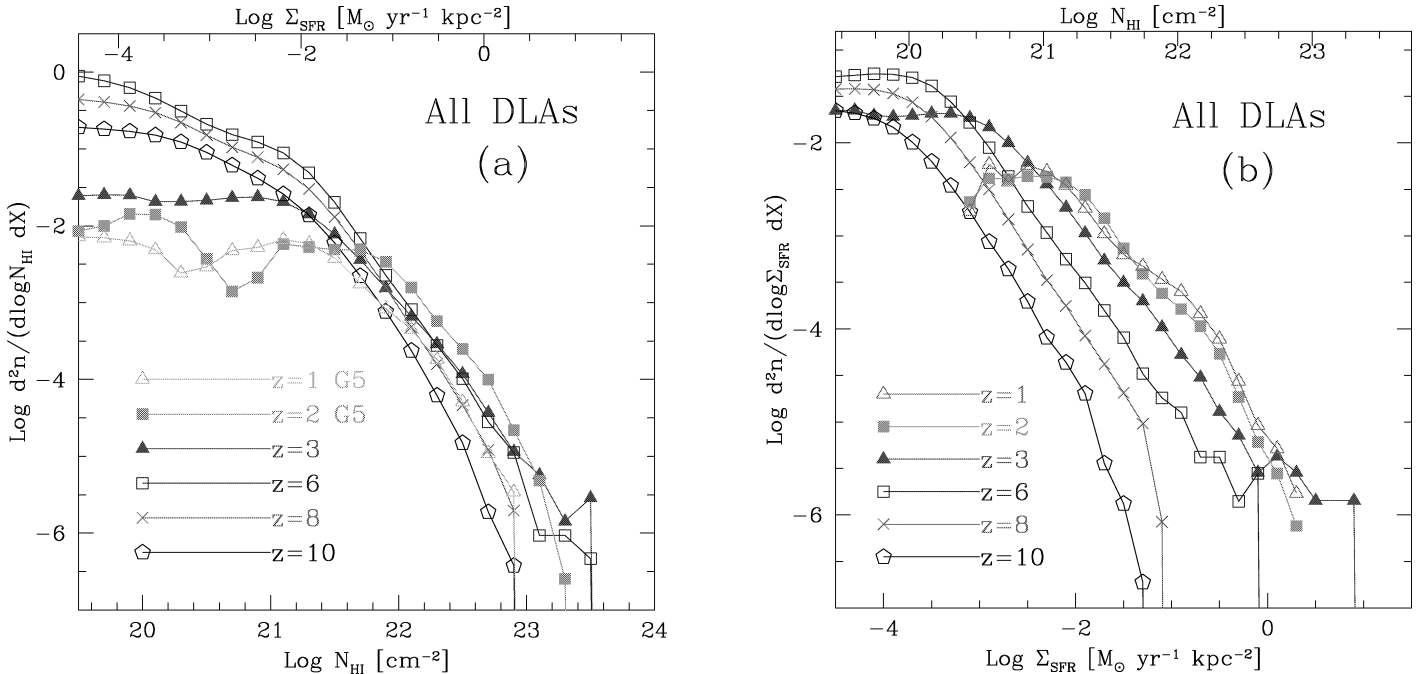


FIG. 1.—Distribution of all DLAs (including both QSO DLAs and GRB-host DLAs) as a function of N_{HI} (a) and Σ_{SFR} (b) at $z = 1$ – 10 . The top axis in each panel indicates corresponding values of N_{HI} and Σ_{SFR} based on the empirical Kennicutt (1998) law. [See the electronic edition of the *Journal* for a color version of this figure.]

al. 2006), and Ly α emitters (Nagamine et al. 2008). In general, the simulations show reasonable agreement with available galaxy observations, giving some confidence that we are capturing the basic aspects of hierarchical galaxy evolution in the context of the Λ CDM model. Moreover, the cosmic star formation history implied by the simulations (Hernquist & Springel 2003) agrees with observational estimates (Faucher-Giguère et al. 2008a) and supports the association of GRBs with massive star formation (Faucher-Giguère et al. 2008b). The adopted cosmological parameters of all simulations considered here are $(\Omega_m, \Omega_b, \Omega_s, \sigma_8, h) = (0.3, 0.7, 0.04, 0.9, 0.7)$, where $h = H_0/(100 \text{ km s}^{-1} \text{ Mpc}^{-1})$.

3. RESULTS

First, we present the distribution of all DLAs in the simulation as a function of N_{HI} in Figure 1a. The method of calculating N_{HI} in the simulations is described fully in Nagamine et al. (2004a). Briefly, we set up a cubic grid that covers each dark matter halo, and calculate N_{HI} by projecting the H I mass distribution onto one of the planes. The quantity “ dn ” is the area covering fraction on the sky along the line element cdt (see eqs. [5]–[7] of Nagamine et al. 2007), and the function $d^2n/(d \log N_{\text{HI}}, dX) = f(N_{\text{HI}}, X)N_{\text{HI}} \ln(10)$ is the “incidence rate” per unit $\log N_{\text{HI}}$ and per unit absorption distance $X(z)$, where $dX = [H_0/H(z)](1+z)^2 dz$. The function $f(N_{\text{HI}}, X)$ is usually referred to as the column density distribution function.

Figure 1a shows that, from $z = 10$ to $z = 6$, the incidence rate increases monotonically with decreasing redshift at all N_{HI} , reflecting the rapidly growing number of dark matter halos. From $z = 6$ to $z = 3$, there is not much change at $\log N_{\text{HI}} > 22$, but the number of columns at $\log N_{\text{HI}} < 21$ has decreased significantly, which could owe to the UV background radiation field imposed at $z = 6$ in the simulation to model reionization. From $z = 3$ to $z = 2$, the number of columns at $\log N_{\text{HI}} > 22$ increases, but it decreases from $z = 2$ to $z = 1$, owing to the conversion of high-density gas into stars.

If long GRBs are associated with the collapse of massive

stars, then their occurrence should be correlated with the local SFR. Therefore we define the following to quantify the distribution of GRB-host DLAs:

$$\zeta_{\text{GRB-host DLA}} \equiv \frac{d^2n}{dX d \log \Sigma_{\text{SFR}}} \frac{\Sigma_{\text{SFR}}}{\langle \Sigma_{\text{SFR}} \rangle} \eta_{\text{GRB}}, \quad (1)$$

where Σ_{SFR} is the projected SFR in units of $(M_\odot \text{ yr}^{-1} \text{ kpc}^{-2})$, and $\langle \Sigma_{\text{SFR}} \rangle$ is a normalization parameter. Although it is somewhat arbitrary, we take $\langle \Sigma_{\text{SFR}} \rangle = 10^{-4}$, because it roughly corresponds to $\log N_{\text{HI}} \approx 20$ based on the Kennicutt (1998) law. The parameter η_{GRB} denotes the mass fraction of stars that become GRBs and have associated afterglows for a given amount of star formation with a certain stellar initial mass function (IMF). The exact value of η_{GRB} depends on the IMF and other GRB physics. Here, we take $\eta_{\text{GRB}} = 10^{-3}$, because the mass fraction of stars with $M > 8 M_\odot$ is 23% of the total for a Chabrier (2003) IMF with a mass range $[0.1, 100] M_\odot$, and the global average of the GRB/SN ratio is $\sim 0.5\%$ (Yoon et al. 2006; Soderberg 2007; Campana et al. 2008). If one takes the number fraction ($\sim 6\%$ for $M > 8 M_\odot$ stars) instead, then $\eta_{\text{GRB}} = 3 \times 10^{-4}$. Here we use the mass fraction, because weighting by $\Sigma_{\text{SFR}}/\langle \Sigma_{\text{SFR}} \rangle$ is done on the basis of stellar mass.

In principle, one could absorb the factor $\langle \Sigma_{\text{SFR}} \rangle$ into η_{GRB} and treat them as one parameter: $\eta'_{\text{GRB}} \equiv \eta_{\text{GRB}}/\langle \Sigma_{\text{SFR}} \rangle$, which would be the GRB rate per projected SFR. However, here we choose to treat them separately to keep the physical meaning of η_{GRB} clear. In the future, GRB theory may be able to estimate the value of η_{GRB} , and observations of GRB-host DLAs will constrain the ratio of $\eta_{\text{GRB}}/\langle \Sigma_{\text{SFR}} \rangle$ (see §§ 4 and 5).

It is worthwhile to look at the distribution $d^2n/(dX d \log \Sigma_{\text{SFR}})$, before weighting it by Σ_{SFR} . Figure 1b shows that the redshift evolution of this distribution is stronger than in Figure 1a. The number of columns with $\log \Sigma_{\text{SFR}} \geq -2.5$ ($\approx \log N_{\text{HI}} \geq 21.0$ for the Kennicutt law) decreases systematically from $z = 1$ to $z = 10$.

Figure 2 shows $\zeta_{\text{GRB-host DLA}}$ as a function of $\log \Sigma_{\text{SFR}}$. Because

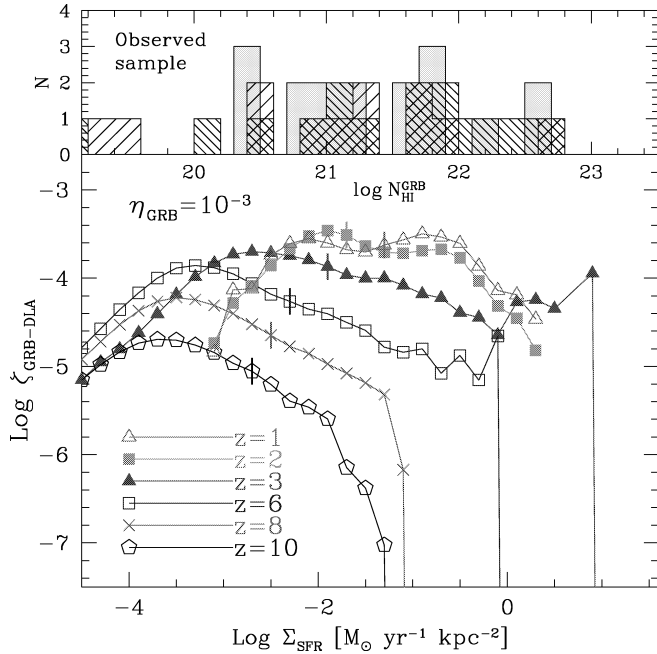


FIG. 2.—Distribution of GRB-host DLAs as a function of Σ_{SFR} and $N_{\text{H I}}^{\text{GRB}}$ at $z = 1$ –10 is shown in the bottom panel. The vertical tick marks indicate the median of the distribution for columns with $\log \Sigma_{\text{SFR}} > -3.0$ or $\log N_{\text{H I}}^{\text{GRB}} > 20.3$. The top panel shows the observed sample of 28 GRB-host DLAs from Chen et al. (2007; broader [finer] hatching for $z < 3$ [$z > 3$]) and 11 GRB-host DLAs from Prochaska et al. (2007; yellow shading; excludes those at $z < 1.6$ with no $N_{\text{H I}}$ measurements). The axis range of $N_{\text{H I}}^{\text{GRB}}$ corresponding to that of Σ_{SFR} is determined from the empirical Kennicutt (1998) law, divided by a factor of 2 to take into account of the fact that the GRB LOSs go through only half of the H I slab on average compared to the QSO LOSs (Prochaska et al. 2007). [See the electronic edition of the Journal for a color version of this figure.]

of the weighting by $\Sigma_{\text{SFR}}/\langle \Sigma_{\text{SFR}} \rangle$, the distribution now exhibits a peak with a broad tail at high Σ_{SFR} . The number of columns with $\log N_{\text{H I}} > 21$ decreases progressively from $z = 1$ to $z = 10$, owing to the decreasing number of massive dark matter halos with deep potential wells toward higher redshifts. This is encouraging for the use of GRB afterglows to probe reionization, because the IGM attenuation signature is less likely to be blocked by the red damping wing of GRB-host DLAs. The median value of the distribution at $\log \Sigma_{\text{SFR}} > -3.0$ ($\approx \log N_{\text{H I}} > 20.3$) is $\log N_{\text{H I}} = 21.4, 21.1, 21.0, 20.7, 20.6,$ and 20.4 for $z = 1, 2, 3, 6, 8,$ and 10 , respectively.

The distributions at $z = 1$ and 2 have broad peaks at $\log N_{\text{H I}} = 21.0$ – 22.3 . The current observed sample (Chen et al. 2007; Prochaska et al. 2007) is shown in the top panel of Figure 2, and observationally there appears to be no indication that $N_{\text{H I}}$ drops toward high- z . If there is any observed trend, it might even be in the opposite sense, and all the observed GRB-host DLAs are at $z \geq 2$. However the current observed sample is still small, and observational selection effects are at play. For example, systems with low $N_{\text{H I}}$ and low metal content are more difficult to identify, especially at higher redshift where the afterglows are typically fainter. We also note that the decline of the distribution at $\log \Sigma_{\text{SFR}} < -2.5$ for $z = 1$ and 2 may owe to the limited resolution of the G5 run compared to the Q5 run.

By integrating $\zeta_{\text{GRB-host DLA}}$ over $\log \Sigma_{\text{SFR}}$, we obtain the “incidence rate” of GRB-host DLAs. The integral at $\log \Sigma_{\text{SFR}} > -3.3$ yields rates of $(6.4, 5.7, 4.4, 1.7, 0.52, 0.14) \times 10^{-4}$ for $z = 1, 2, 3, 6, 8,$ and 10 , respectively, for the assumed value of $\eta_{\text{GRB}}/\langle \Sigma_{\text{SFR}} \rangle = 10$. Figure 3 compares the derived incidence

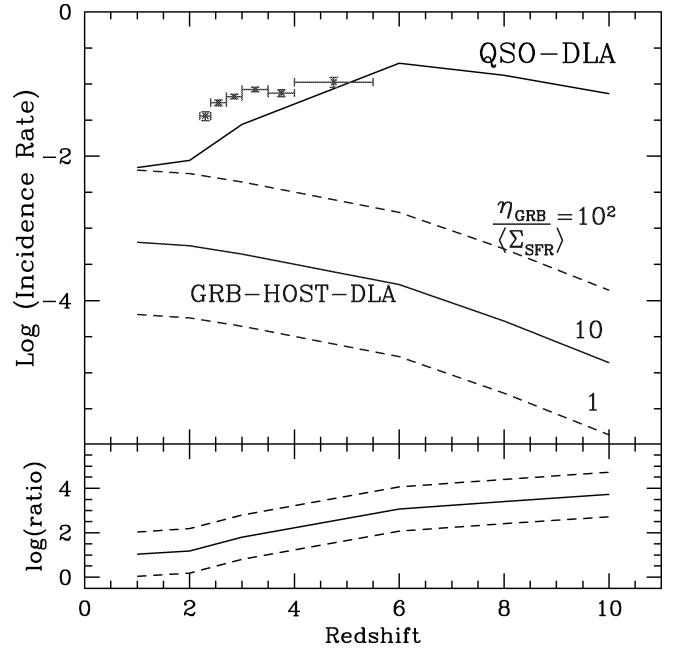


FIG. 3.—Top panel: Incidence rates of GRB-host DLAs and QSO DLAs as a function of redshift. (See text for the source of the data points.) For GRB-host DLAs, the three blue curves correspond to $\eta_{\text{GRB}}/\langle \Sigma_{\text{SFR}} \rangle = 10^2, 10,$ and 1 from top to bottom. Bottom panel: Ratio of the two incidence rates. [See the electronic edition of the Journal for a color version of this figure.]

rate of GRB-host DLAs to that of QSO DLAs. The red data points are the updated version⁴ of Prochaska et al. (2005) using SDSS DR5. Our simulations somewhat underpredict the QSO-DLA incidence rate owing to the underestimate of $f(N_{\text{H I}})$ at $\log N_{\text{H I}} < 21$ (Nagamine et al. 2004a). There is a stark difference between the evolution of the two rates: the incidence rate of GRB-host DLAs decreases monotonically toward high- z , whereas the QSO-DLA rate increases from $z = 1$ to $z = 6$. This is because we assumed that GRBs are correlated with star formation and their distribution is not random, unlike the background quasars. The offset between the two rates tells us about the difference between the total H I cross section of galaxies and the area covering fraction of star-forming regions. The QSO-DLA sight lines can also probe the outskirts of galaxies where star formation is nonexistent; therefore their incidence rate is much higher than that of GRB-host DLAs.

4. PROBABILITY FOR A GIVEN GRB

Of immediate interest to GRB observers is the chance probability of finding a GRB-host DLA for a given GRB event. For individual GRBs, the probability of having a GRB-host DLA should depend on the geometry of the H I gas distribution around the GRB along the LOS. While our simulations do not have the resolution to follow the gas dynamics within molecular clouds, the Q5 run has a physical gravitational softening length of 0.31 (0.18) h^{-1} kpc at $z = 3$ (6), and the gas distribution above these scales is followed reasonably well. The O and B stars would have ionized all the gas within ~ 100 pc of the GRB creating an H II region; thus we expect the DLA gas to be located at > 0.1 kpc from the GRB (Prochaska et al. 2007). Then, our simulations can follow the qualitative trend in the redshift evolution of the incidence rate of GRB-host DLAs.

Since our simulations roughly match the Kennicutt law (Nagamine et al. 2004b), it is guaranteed that columns with

⁴ See <http://www.ucolick.org/~xavier/SDSSDLA/>.

$\log N_{\text{H I}} > 20.3$ will have star formation along the LOS. Therefore if long GRBs are associated with star formation as we have assumed, most of the GRB LOSs will have a high- $N_{\text{H I}}$ gas in their host galaxy, the majority of which are GRB-host DLAs. A more detailed analysis would be required to fully confirm this, by generating the absorption-line profiles for each GRB LOS, and we plan to examine this in due course using higher resolution simulations.

Nevertheless, Figure 2 shows that the number of high- $N_{\text{H I}}$ systems decreases with increasing redshift, and so we expect that the chance probability of having a high- $N_{\text{H I}}$ DLA for a given GRB event will also decline toward high z with a similar qualitative trend as shown in Figure 3. But we stress that the incidence rate shown in Figure 3 is *not* the probability of detecting a DLA for a given GRB.

5. CONCLUSIONS AND DISCUSSION

Using cosmological SPH simulations, we have examined the redshift evolution of incidence rates of GRB-host DLAs, assuming that long GRBs are correlated with local SFR. The distribution of GRB-host DLAs is intrinsically different from that of QSO DLAs, and the incidence rate of GRB-host DLAs decreases monotonically toward high z , whereas that of QSO DLAs increases from $z = 1$ to $z = 6$. Quasars are assumed to be randomly distributed background sources in the sky, which illuminate the DLA gas in foreground galaxies. GRBs can also serve as randomly distributed beacons with respect to the DLA gas in foreground galaxies, but for GRB-host DLAs, GRBs are not random background sources because they are in the same host galaxy.

We find that the incidence rate of GRB-host DLAs with $\log N_{\text{H I}} > 21.0$ decreases rapidly at $z \geq 6$, suggesting that the likelihood of observing the IGM attenuation signature in GRB afterglows increases toward higher redshifts, without being blocked by the red damping of DLAs in the GRB host galaxies. This enhances the prospects for using high- z GRBs to probe the reionization history of the universe. Our predictions can be tested by upcoming high- z GRB missions, including *JANUS* (*Joint Astrophysics Nascent Universe Scout*) and *SVOM* (*Space multiband Variable Object Monitor*).

It might be hoped that it would be possible to estimate the incidence rate of GRB-host DLAs by accumulating a large GRB sample. However, because GRBs are not random background sources for GRB-host DLAs, this would require a prohibitively large GRB sample to estimate the area covering fraction of GRB-host DLAs from GRB observations alone. If long GRBs do indeed trace star-forming regions, and if all the LOSs to star-forming regions are coincident with DLAs, then one could estimate the total GRB-host-DLA incidence rate simply by measuring the area covering fraction of star-forming regions from deep imaging surveys of galaxies. When the number of GRBs becomes comparable to that of QSOs, one should expect nonnegligible new intervening DLAs in GRB LOSs that are not associated with GRB hosts, since GRB afterglows now act as random beacons.

An alternative possibility would be to search for quasars in the proximity of GRBs, or vice versa. Such a search of QSO-GRB pair LOSs would yield a coincidence probability between QSO DLAs and GRB-host DLAs, which roughly corresponds to the ratio of the two incidence rates. For this purpose, only those systems for which the QSOs are in the background and the GRBs in the foreground can be used. So far, no such cases have been identified, but a combination of all-sky GRB surveys (e.g., BATSE, *Swift*, *GLAST*) and optical-IR imaging surveys of galaxies (e.g., SDSS, Pan-STARRS, LSST) may prove successful in the future. A constraint on the ratio of the two incidence rates would make it possible to estimate the ratio $\eta_{\text{GRB}}/\Sigma_{\text{SFR}}$. In addition, deep observations of GRB host galaxies could constrain Σ_{SFR} independently. Then combining the above two constraints would allow us to estimate the value of η_{GRB} .

This work is supported in part by the National Aeronautics and Space Administration under grant/cooperative agreement NNX08AE57A issued by the Nevada NASA EPSCoR program and the President's Infrastructure Award from UNLV. B. Z. acknowledges the support from the NASA grant NNG06GH62G. We acknowledge the significant contribution of Volker Springel for the simulations used in this work. K. N. is grateful for the hospitality of the Institute for the Physics and Mathematics of the Universe, the University of Tokyo, where part of this work was done.

REFERENCES

- Barkana, R., & Loeb, A. 2004, *ApJ*, 601, 64
 Berger, E., et al. 2006, *ApJ*, 642, 979
 Campana, S., et al. 2008, *ApJ*, 683, L9
 Chabrier, G. 2003, *PASP*, 115, 763
 Chen, H.-W., et al. 2007, *ApJ*, 667, L125
 Ciardi, B., & Loeb, A. 2000, *ApJ*, 540, 687
 Cusumano, G., et al. 2006, *Nature*, 440, 164
 Davé, R., et al. 1999, *ApJ*, 511, 521
 Fan, X., Carilli, C. L., & Keating, B. 2006, *ARA&A*, 44, 415
 Faucher-Giguère, C.-A., et al. 2008a, *ApJ*, submitted (arXiv:0807.4177)
 ———. 2008b, *ApJ*, 682, L9
 Gou, L. J., et al. 2004, *ApJ*, 604, 508
 Haislip, J. B., et al. 2006, *Nature*, 440, 181
 Hernquist, L., & Springel, V. 2003, *MNRAS*, 341, 1253
 Holder, G. P., et al. 2003, *ApJ*, 595, 13
 Inoue, S., Omukai, K., & Ciardi, B. 2007, *MNRAS*, 380, 1715
 Katz, N., Weinberg, D. H., & Hernquist, L. 1996, *ApJS*, 105, 19
 Kawai, N., et al. 2006, *Nature*, 440, 184
 Kennicutt, R. C., Jr. 1998, *ApJ*, 498, 541
 Lamb, D. Q., & Reichart, D. E. 2000, *ApJ*, 536, 1
 McQuinn, M., et al. 2008, *MNRAS*, 388, 1101
 Miralda-Escudé, J. 1998, *ApJ*, 501, 15
 Nagamine, K., et al. 2004a, *MNRAS*, 348, 421
 Nagamine, K., et al. 2004b, *MNRAS*, 348, 435
 ———. 2004c, *MNRAS*, 350, 385
 ———. 2006, *ApJ*, 653, 881
 ———. 2007, *ApJ*, 660, 945
 ———. 2008, *ApJ*, submitted (arXiv:0802.0228)
 Night, C., et al. 2006, *MNRAS*, 366, 705
 Paczyński, B. 1998, *ApJ*, 494, L45
 Prochaska, J. X., et al. 2005, *ApJ*, 635, 123
 ———. 2007, *ApJ*, 666, 267
 Ruiz-Velasco, A. E., et al. 2007, *ApJ*, 669, 1
 Soderberg, A. M. 2007, in *AIP Conf. Proc.* 937, *Supernova 1987A: 20 Years After: Supernovae and Gamma-Ray Bursters*, ed. S. Immler & R. McCray (New York: AIP), 492
 Springel, V. 2005, *MNRAS*, 364, 1105
 Springel, V., & Hernquist, L. 2003a, *MNRAS*, 339, 289
 ———. 2003b, *MNRAS*, 339, 312
 Totani, T. 1997, *ApJ*, 486, L71
 Totani, T., et al. 2006, *PASJ*, 58, 485
 Vreeswijk, P. M., et al. 2004, *A&A*, 419, 927
 Watson, D., et al. 2006, *ApJ*, 652, 1011
 Woosley, S. E. 1993, *ApJ*, 405, 273
 Yoon, S.-C., Langer, N., & Norman, C. 2006, *A&A*, 460, 199